Chemistry of Coordinatively Unsaturated Bis(thiolato)ruthenium(II) Complexes (η^6-arene)Ru(SAr)$_2$ [SAr = 2,6-Dimethylbenzenethiolate, 2,4,6-Triisopropylbenzenethiolate; (SAr)$_2$ = 1,2-Benzenedithiolate; Arene = Benzene, *p*-Cymene, Hexamethylbenzene]

Kazushi Mashima,*,† Hiromu Kaneyoshi,‡ Sei-ichi Kaneko,† Aki Mikami,‡ Kazuhide Tani,† and Akira Nakamura‡

Department of Chemistry, Faculty of Engineering Science, Osaka University, Toyonaka, Osaka 560, Japan, and Department of Macromolecular Science, Faculty of Science, Osaka University, Toyonaka, Osaka 560, Japan

Received September 3, 1996⊗

Mononuclear 16-electron arene−ruthenium(II)−thiolate complexes of the general formula (η^6-arene)Ru(SAr)$_2$ (**2**, Ar = 2,6-$C_6H_3Me_2$ = Xyl; **3**, Ar = 2,4,6-$C_6H_2(CHMe_2)_3$; arene = C_6H_6 (**a**), arene = *p*-$MeC_6H_4(CHMe_2)$ = *p*-cymene (**b**), arene = C_6Me_6 (**c**)) have been prepared by treatment of [(η^6-arene)$RuCl_2$]$_2$ (**1**) with the corresponding sodium arenethiolate in methanol. Reaction of **2b** with disodium of 1,2-benzenedithiolate (=$S_2C_6H_4$) led to a mixture of monomer and dimer complexes (η^6-*p*-cymene)Ru($S_2C_6H_4$) (**4b**) and [(η^6-*p*-cymene)Ru($S_2C_6H_4$)]$_2$ (**5b**) in solution. A complex (η^6-C_6Me_6)Ru($S_2C_6H_4$) (**4c**) was predominantly monomeric, revealed by a crystal structure analysis of **4c**. All these monomeric complexes show intense blue color of the LMCT band due to the donation from the filled S(pπ) orbital to the empty Ru(dπ*) orbital, which stabilizes coordinatively unsaturated ruthenium(II). The structures of these complexes are characterized by NMR and mass spectra and elemental analysis in addition to the X-ray crystal structure determinations of **2a**,**b**, **3c**, and **4c**, indicating the two-legged piano stool geometry. The newly prepared 16-electron complexes react with π-accepting molecules such as isocyanide, carbon monoxide, and trialkylphosphine. Treatment of **2b** with an excess of *tert*-butyl isocyanide resulted in the release of the *p*-cymene ligand to give *trans*-Ru(SXyl)$_2$(CN^tBu)$_4$ (**8**). Similarly, reaction of **5b** with an excess of *tert*-butyl isocyanide afforded *cis*-Ru($S_2C_6H_4$)(CN^tBu)$_4$ (**10**), while reaction of **5b** with 6 equiv of *tert*-butyl isocyanide gave a binuclear complex [Ru($S_2C_6H_4$)(CN^tBu)$_3$]$_2$ (**11**). In the case of more strongly coordinating C_6Me_6 derivatives **2c** and **4c**, one molecule of *tert*-butyl isocyanide can coordinate to the ruthenium atom, resulting in the formation of (η^6-C_6Me_6)Ru(SXyl)$_2$(CN^tBu) (**9c**) and (η^6-C_6Me_6)Ru($S_2C_6H_4$)(CN^tBu) (**12c**), respectively. Reactions of **5b** and **4c** with an excess of triethylphosphine afforded (η^6-*p*-cymene)Ru($S_2C_6H_4$)(PEt_3) (**13b**) and (η^6-C_6Me_6)Ru($S_2C_6H_4$)-(PEt_3) (**13c**), respectively. In the carbonylation, **2b** gave a binuclear carbonyl complex $(CO)_3Ru(\mu$-SXyl$)_3Ru(CO)_2$(SXyl) (**14**), while the carbonylation of the C_6Me_6 complex **2c** afforded (η^6-C_6Me_6)Ru(SXyl)$_2$(CO) (**15**). Versatile reactivity of 16-electron ruthenium(II) thiolate complexes is thus demonstrated.

Introduction

The majority of organometallic complexes of the late and middle transition metals are isolated as 18-electron species, while the corresponding 16-electron species are more reactive sometimes causing catalysis. These species have thus attracted recent interest. It is becoming a trend that π donation by a lone pair on the coordinating atom alleviates such electron deficiency and coordinative unsaturation around the transition metal center. A thiolate ligand possesses a σ-donor orbital along with lone-pair orbitals that have the correct symmetry for π-interaction with a metal d orbital. Actually it has been demonstrated that some of the bulky thiolate ligands effectively stabilize coordinatively unsaturated mononuclear complexes. Koch *et al*. have reported the synthesis and structures of pentacoordinated ruthenium(IV) thiolate complexes having trigonal bipyramidal geometry, *i.e.*, Ru(S-2,3,5,6-Me_4C_6H)$_4$-($NCCH_3$) and [Ru(S-2,3,5,6-Me_4C_6H)$_3$($NCCH_3$)$_2$]$^+$.[1−3] Recently Maitlis *et al*. have reported half-sandwich iridium complexes such as Cp*Ir(SC_6F_4H-*p*)$_2$ and Cp*Ir(SC_6F_5)$_2$, which are 16-electron and have coordinatively unsaturated structure.[4−6] Bergman *et al*. have recently prepared and characterized 16-electron mononuclear os-

† Department of Chemistry, Faculty of Engineering Science.
‡ Department of Macromolecular Science, Faculty of Science.
⊗ Abstract published in *Advance ACS Abstracts,* February 1, 1997.

(1) Miller, M.; O'Sullivan, T.; Vries, N. d.; Koch, S. A. *J. Am. Chem. Soc.* **1985**, *107*, 3714.
(2) Koch, S. A.; Millar, M. *J. Am. Chem. Soc.* **1983**, *105*, 3362.
(3) Satsangee, S. P.; Hain, J. H., Jr.; Cooper, P. T.; Koch, S. A. *Inorg. Chem.* **1992**, *31*, 5160.
(4) Garcia, J. J.; Torrens, H.; Adams, H.; Bailey, N. A.; Maitlis, P. M. *J. Chem. Soc., Chem. Commun.* **1991**, 74.
(5) Garcia, J. J.; Torrens, H.; Adams, H.; Bailey, N. A.; Scacklady, A.; Maitlis, P. M. *J. Chem. Soc., Dalton Trans.* **1993**, 1529.

S0276-7333(96)00759-5 CCC: $14.00

mium(II) complexes (η^6-*p*-cymene)Os$(SR)_2$ (R = *tert*-butyl, 2,6-dimethylphenyl, and 2,4,6-trimethylphenyl).[7,8] These complexes are expected to be still reactive toward a wide variety of π-donative molecules.

We describe details of the preparation, properties, and crystal structures of mononuclear 16-electron ruthenium(II) complexes of general formula (η^6-arene)Ru$(SAr)_2$ [SAr = 2,6-dimethylbenzenethiolate, SAr = 2,4,6-tri(isopropyl)benzenethiolate, $(SAr)_2$ = 1,2-benzenedithiolate], as well as their inherent reactivity including replacement of the labile arene ligand. A part of this work has been the subject of a preliminary communication.[9]

Results and Discussion

Synthesis and Properties. The mononuclear 16-electron ruthenium(II) complexes of general formula (η^6-arene)Ru$(SAr)_2$ [SAr = 2,6-dimethylbenzenethiolate = SXyl (**2**), SAr = 2,4,6-tri(isopropyl)benzenethiolate (**3**), $(SAr)_2$ = 1,2-benzenedithiolate (**4**); arene = C_6H_6 (**a**), *p*-$CH_3C_6H_4(CHMe_2)$ (**b**), C_6Me_6 (**c**)] can be isolated as deep blue, air-sensitive solids in good to modest yield. Addition of [(η^6-C_6H_6)$RuCl_2]_2$ (**1a**) to a solution of 1.5-fold excess of sodium 2,6-dimethylbenzenethiolate in methanol resulted in the rapid precipitation of (η^6-C_6H_6)Ru$(SXyl)_2$ (**2a**) as deep blue microcrystals in 71% yield (eq 1). More than 1.5-fold excess of the thiolate is

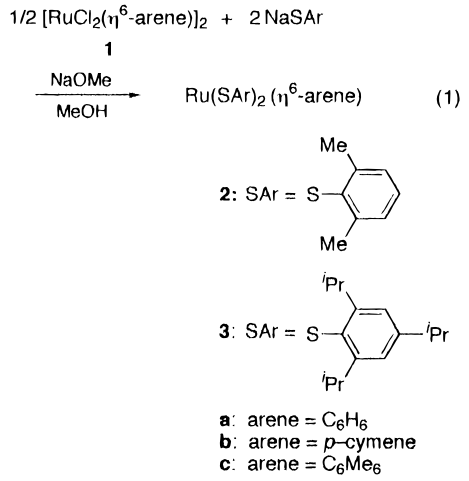

required to achieve high chemical yield, while reaction of **1a** with 4 equiv of the thiolate afforded **2a** in poor yield (ca. 10%). Complexes **2b**[9] and **2c** were isolated similarly by the reaction of sodium 2,6-dimethylbenzenethiolate with [(η^6-*p*-cymene)$RuCl_2]_2$ (**1b**) and [(η^6-C_6Me_6)$RuCl_2]_2$ (**1c**), respectively. The same synthetic method using the sodium salt of 2,4,6-triisopropylbenzenethiolate can be applied for the synthesis of complexes **3a**−**c**.

On the basis of the ^{1}H NMR spectra of **2** and **3**, the ratio of η^6-arene ligand and thiolate ligand was strictly 1:2. The two thiolate ligands are magnetically equivalent, which is in contrast to the solid-state structure determined by X-ray analysis (*vide infra*). The ^{1}H NMR spectra of **2a** and **3a** displayed a singlet at δ 4.87 and 4.92, respectively, assignable to the η^6-coordinated benzene ligand in addition to the signals due to two thiolate ligands. Aromatic protons of *p*-cymene in **2b** and **3b** were observed as the AX pattern of para-substituted aromatic protons. The ^{1}H NMR spectra of **2c** and **3c** showed a singlet at δ 1.91 and 1.86, respectively, due to η^6-C_6Me_6 ligand. The FAB mass spectra of **2** and **3** show parent ions, but the exception was **3a** whose FAB mass spectrum gave a fragmented peak due to the loss of one thiolate ligand. The color of the isolated complexes is deep blue, and their λ_{max} values in electronic spectra lie in the range 660−715 nm. Such an intense blue color corresponds to the LMCT band of coordinatively unsaturated ruthenium(II) complexes Cp*RuCl[P(^{i}Pr)$_3$],[10] Cp*RuI[PPh(^{i}Pr)$_2$],[11] [Cp*Ru(μ-OMe)$]_2$,[12−14] [Cp*Ru(μ-SR)$]_2$,[15,16] [(η^6-C_6H_6)-Ru(μ-$NC_6H_3(^i$Pr)$_2$-2,6)$]_2$,[17] and Ru$(SC_6F_5)_2(PPh_3)_2$,[18] as well as the related Cr,[19] Mo,[20,21] Re,[22] Os[7,8] and Ir,[4,5] complexes, in which a filled π-orbital of sulfur atom donates some electron density to a vacant d-oribtal of the metal as already pointed out for 16-electron half-sandwich transition metal complexes.[23,24] Thus, the analytical and spectroscopic data support the formulation as mononuclear 16-electron ruthenium(II) thiolate complexes, and this formulation has been confirmed in the case of **2a**, **2b**,[9] and **3c** by X-ray structural analysis (*vide infra*).

Although sterically less demanding thiolate ligands have a tendency to form bridges between unsaturated metal centers,[25] 1,2-benzenedithiolate complex **4c** was also formed as black crystals in 46% yield by reaction of the disodium salt of 1,2-benzenedithiolate with **2c** in THF (eq 2). The reaction of the disodium salt with [(η^6-C_6Me_6)$RuCl_2]_2$ (**1c**) also afforded **4c** but resulted in contamination with unidentified complexes. The ^{1}H NMR spectrum of **4c** displayed the AA′XX′ pattern due to the 1,2-benzenedithiolate moiety and a singlet at δ 2.37 due to the η^6-C_6Me_6 ligand, the relative intensity being 1:1. The chemical shift value of η^6-C_6Me_6 in **4c** moved unexpectedly to lower field as compared with **1c**, **2c**, and **3c**. This may be attributed to the large donation

(6) Klein, D. P.; Kloster, G. M.; Bergman, R. G. *J. Am. Chem. Soc.* **1990**, *112*, 2022.
(7) Michelman, R. I.; Andersen, R. A.; Bergman, R. G. *J. Am. Chem. Soc.* **1991**, *113*, 5100.
(8) Michelman, R. I.; Ball, G. E.; Bergman, R. G.; Andersen, R. A. *Organometallics* **1994**, *13*, 869.
(9) Mashima, K.; Mikami, A.; Nakamura, A. *Chem. Lett.* **1992**, 1473.
(10) Campion, B. K.; Heyn, R. H.; Tilley, T. D. *J. Chem. Soc., Chem. Commun.* **1988**, 278.
(11) Johnson, T. J.; Folting, K.; Streib, W. E.; Martin, J. D.; Huffman, J. C.; Jackson, S. A.; Eisenstein, O.; Caulton, K. G. *Inorg. Chem.* **1995**, *34*, 488.
(12) Kölle, U.; Kossakowski, J. *J. Chem. Soc., Chem. Commun.* **1988**, 549.
(13) Koelle, U.; Kossakowski, J. *J. Organomet. Chem.* **1989**, *362*, 383.
(14) Loren, S. D.; Campion, B. K.; Heyn, R. H.; Tilley, T. D.; Bursten, B. E.; Luth, K. W. *J. Am. Chem. Soc.* **1989**, *111*, 4712.
(15) Koelle, U.; Rietmann, C.; Englert, U. *J. Organomet. Chem.* **1992**, *423*, C20.
(16) Takahashi, A.; Mizobe, Y.; Matsuzaka, H.; Dev, S.; Hidai, M. *J. Organomet. Chem.* **1993**, *456*, 243.
(17) Kee, T. P.; Park, L. Y.; Robbins, J.; Schrock, R. R. *J. Chem. Soc., Chem. Commun.* **1991**, 121.
(18) Catala, R.-M.; Cruz-Garritz, D.; Sosa, P.; Terreros, P.; Torrens, H.; Hills, A.; Hughes, D. L.; Richards, R. L. *J. Organomet. Chem.* **1989**, *359*, 219.
(19) Sellmann, D.; Ludwig, H.; Huttner, G.; Zsolnai, L. *J. Organomet. Chem.* **1985**, *294*, 199.
(20) Ashby, M. T.; Enemark, J. H. *J. Am. Chem. Soc.* **1986**, *108*, 730.
(21) Cleland, W. E., Jr.; Barnhart, K. M.; Yamanouchi, K.; Collison, D.; Mabbs, F. E.; Ortega, R. B.; Enemark, J. H. *Inorg. Chem.* **1987**, *26*, 1017.
(22) Chang, L.; Aizawa, S.; Heeg, M. J.; Deutsch, E. *Inorg. Chem.* **1991**, *30*, 4920.
(23) Hofmann, P. *Angew. Chem., Int. Ed. Engl.* **1977**, *8*, 536.
(24) Siedle, A. R.; Newmark, R. A.; Pignolet, L. H.; Wang, D. X.; Albright, T. A. *Organometallics* **1986**, *5*, 38.
(25) Dance, I. G. *Polyhedron* **1986**, *5*, 1037.

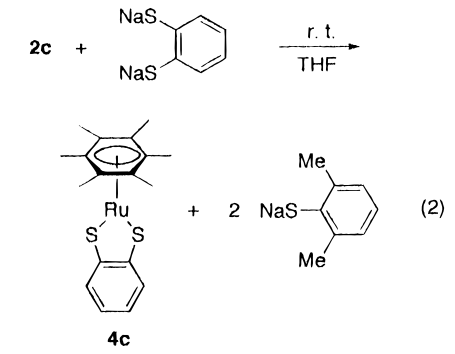

from the S(pπ) orbitals. The electronic spectrum of **4c** exhibited a characteristic LMCT band at 563 nm, indicating **4c** as a mononuclear 16-electron complex. The structure of **4c** was further revealed by X-ray analysis (*vide infra*).

In sharp contrast to the case of **4c**, reaction of the disodium salt of 1,2-benzenedithiolate with **2b** in THF resulted in the formation of an orange dimeric complex **5b** (eq 3). FAB mass spectra of **5b** showed a parent peak

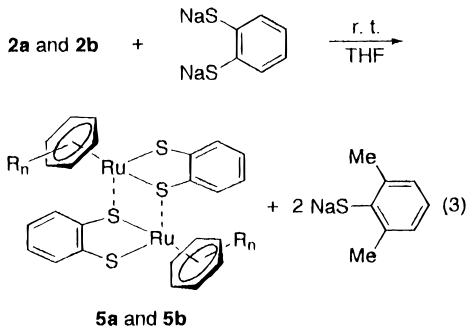

at *m*/*z* 751, corresponding to a dimeric structure of **5b**. The ^{1}H NMR spectrum of **5b** in $CDCl_3$ at 30 °C displayed two sets of proton signals; one set of four nonequivalent protons of 1,2-benzenedithiolate is attributed to the dimer **5b**, and the other has an AA′BB′ pattern due to protons of 1,2-benzenedithiolate of the monomeric complex **4b** similar to **4c**. Such thiolate-bridged dimer structures have been reported for benzenedithiolate complexes, *i.e.*, $[Cp^*Ru(\mu\text{-}S_2C_6H_4)]_2$,[26] rhodium (**6**)[27] and iron (**7**).[28] Similar reaction of the disodium salt of 1,2-benzenedithiolate with **2a** in THF afforded **5a** in 48% yield, which was also in equilibrium with its monomer **4a**.

The ratio of **4b** and **5b** in solution depends on the temperature, indicating an equilibrium between the dimer and the monomer. This equilibrium in C_6D_6 was monitored by ^{1}H NMR spectroscopy to give K_{diss} at various temperature (30−60 °C). Thus the plot affords parameters $\Delta H° = 8.74 \pm 2.22$ (kJ/mol) and $\Delta S° = 138 \pm 7$ (J mol^{-1} K^{-1}). Exceedingly low solubility of **5a** in most organic solvents prevented the equilibrium measurement for **5a**.

Crystal Structures of 2a,b, 3c, and 4c. The monomeric structure of **3c** is provided in Figure 1. Selected bond distances and angles and torsion angles are listed in Table 1. The X-ray analysis of **2a**,**b**[9] confirmed that they have essentially the same structure

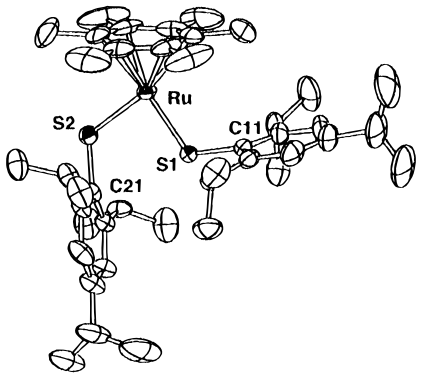

Figure 1. ORTEP drawing of **3c** with the numbering scheme.

Table 1. Selected Bond Distances and Angles for 2a,b, 3c, and 4c[a]

	2a	2b	3c	4c
	Bond Distances (Å)			
Ru−S1	2.269(7)	2.263(7)	2.259(1)	2.263(1)
Ru−S2	2.292(9)	2.311(6)	2.339(1)	2.256(1)
Ru−CEN	1.686	1.673	1.702	1.684
S1−C11	1.83(3)	1.82(2)	1.791(4)	1.741(4)
S2−C21	1.78(2)	1.77(2)	1.777(4)	1.750(5)
	Bond Angles (deg)			
Ru−S1−C11	108.1(8)	108.9(8)	113.8(1)	106.7(2)
Ru−S2−C21	114(1)	114.2(8)	114.4(1)	106.8(2)
S1−Ru−S2	88.0(3)	89.0(1)	86.74(4)	87.1(1)
S1−Ru−CEN	141	140	145.0	137.0
S2−Ru−CEN	131	131	128.2	135.8
	Torsion Angles (deg)			
S2−Ru−S1−C11	178(1)	174(1)	175.5(2)	3.9(2)
CEN−Ru−S1−C11	0	1	1.1	172.7
S1−Ru−S2−C21	11(1)	3(1)	24.5(2)	3.4(2)
CEN−Ru−S2−C21	166.9	172	152.9	173.3

[a] CEN = the centroid of aromatic ring carbons, C1−C6, of the ligand.

as **3c**, and only the selected bond distances and angles for **2a**,**b** are given in Table 1. Thus the introduction of higher bulky substituents at the ortho-position of the benzenethiolate ligand did not greatly affect the geometry around ruthenium atom in **3c**.

In these complexes, the coordination geometry around the ruthenium atom is best described as a two-legged piano stool. Thus the plane defined by the centroid of η^6-benzene, two sulfur atoms, and a ruthenium atom is exactly planar; the angle sum for the ruthenium atom is 360°. This is consistent with the preference that the presence of a π-donor ligand stabilizes a planar structure comprised of the centroid of Cp ligand, the ruthenium atom, and the two ligands for CpRu(L)(L′).[11] The most intriguing feature of these complexes is an "*endo-exo*" conformation **B** which is schematically shown in Chart 1 together with two other possible conformations **A** and **C**. In conformation **B**, one aromatic substituent is turned away from the η^6-benzene ligand so as to minimize steric interaction, while the other is twisted toward it. Noteworthy is that this twisted conformation **B** has been observed even for complex **3c** where exist sterically bulky C_6Me_6 and 2,4,6-triisopropylbenzenethiolate ligands. In complexes **2a,b** and **3c**, an Ru−S1 bond distance (2.263(7)−2.269(7) Å) in *exo*-orientation is shorter than the other Ru−S2 bond distance (2.292(9)−2.311(6) Å) in *endo*-orientation, while the bond distance of S1−C11 (1.82(2)−1.83(3) Å) is longer than that of S2−C21 (1.77(2)−1.78(2) Å). The Ru−S1−C11 bond angles (108.1(8) and 108.9(8)°) of **2a**,**b** are smaller

(26) Hörnig, A.; Englert, U.; Kölle, U. *J. Organomet. Chem.* **1994**, *464*, C25.
(27) Russell, M. J. H.; White, C.; Yates, A.; Maitlis, P. M. *J. Chem. Soc., Dalton Trans.* **1978**, 849.
(28) Kang, B. S.; Weng, L. H.; Wu, D. X.; Wang, F.; Guo, Z.; Huang, L. R.; Huang, Z. Y.; Liu, H. Q. *Inorg. Chem.* **1988**, *27*, 1128.

Chart 1

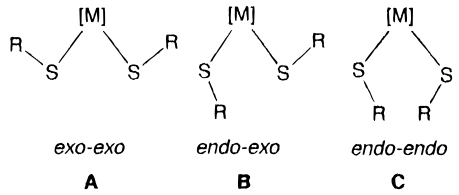

than the Ru−S2−C21 bond angles (114(1) and 114.2(8)°), while **3c** has almost the same bond angles of Ru−S1−C11 (113.8(1)°) and Ru−S1−C11 (114.4(1)°) due to the bulkiness between the C_6Me_6 ligand and the *exo*-oriented 2,4,6-triisopropylbenzenethiolate ligand. These observations correspond to the larger contribution of the pπ orbital on the sulfur atom in an *exo*-oriented ligand to the ruthenium atom rather than that of the other *endo*-oriented ligand. The bond lengths and angles found within the aromatic ligand show no unusual features.

The crystal structure of **4c** is shown in Figure 2. In this chelating thiolate complex **4c**, the *endo-endo* conformation **C** is obviously taken. Here, the most intriguing feature is higher coordinative unsaturation around the ruthenium atom compared with the *endo-exo* or *exo-exo* isomer. To alleviate this, the donative interaction from pπ orbitals on sulfur occurs due to the conjugation with arene orbitals to stabilize the coordinatively unsaturated ruthenium center in **4c**, and the Ru−S bond distances thereby are 2.263(1) and 2.256(1) Å, both being shorter than that of the *endo*-oriented Ru−S bond found for **2a**,**b** and **3c** but comparable to that of the *exo*-oriented Ru−S bond in **2a**,**b** and **3c**. The S−C bond distances (1.741(4) and 1.750(5) Å) are shorter than those found for **2a**,**b**, **3c**, and 16-electron $[Cr(CO)_3(1,2\text{-}S_2C_6H_4)]^{2-}$.[19] These bond distances are similar to those of 1,2-benzenedithiolate complexes of Fe,[29,30] Mo,[31−33] W,[34] Nb,[35] and Zr,[36] being consistent with some contribution of S=C double-bond character as witnessed by the comparison with the double-bonded S=C distance of 1.67(2)−1.75(1) Å in thiourea derivatives.[37]

The summation of angles around the ruthenium atom of **4c** defined by the centroid of η^6-C_6Me_6 and two sulfur atoms is 359.9°, indicating the highly planar geometry around the ruthenium atom. The fold angle between the best planes defined by aromatic carbon atoms of C_6Me_6 and 1,2-benzenedithiolate is 81.79°, and thus the $S_2C_6H_4$ plane is bent from the RuS_2 plane as already observed for 1,2-benzenedithiolate complexes of transition metals.[31,35]

Comparative M−S bond distances and M−S−C bond angles for 16-electron ruthenium thiolate complexes and the known $L_nM(SR)_2$ type thiolate complexes are listed in Table 2. The configuration of "$M(SR)_2$" fragments

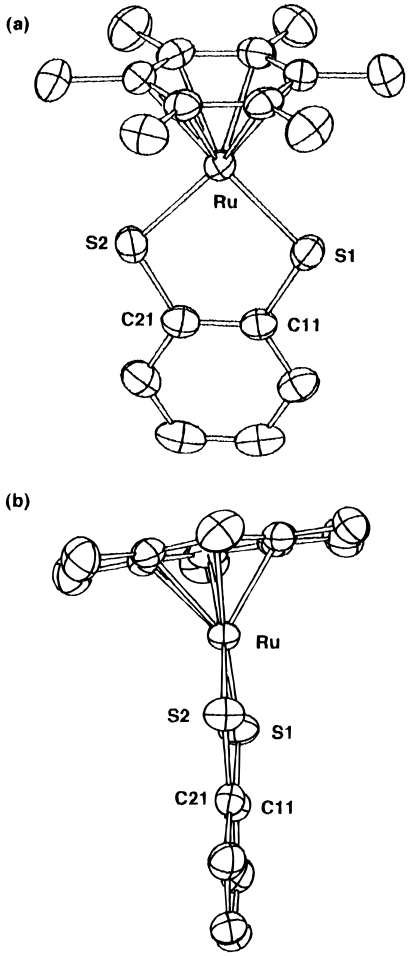

Figure 2. ORTEP drawings of **4c** with the numbering scheme: (a) front view; (b) side view.

varied according to the orientation of metal dπ and sulfur pπ orbitals as well as the geometry around metal center. It is noteworthy that the conformation **B** in Chart 1 is predominantly adopted by the known pentacoordinated thiolate complexes as well as by many of the hexacoordinated electron deficient thiolate complexes[21,38] except for the "*exo-exo*" conformation **A** of $CpMo(NO)(SPh)_2$[20] and $Cp^*Ir(SC_6F_5)_2$.[5] In the pentacoordinated complexes in Table 2 with conformation **B**, the *exo*-oriented thiolate ligand has shorter M−S and the longer S−C bond distances than those of the *endo*-oriented one.

Reactivity. The 16-electron organometallic complexes of transition metals readily react with diverse π-acceptor molecules such as PR_3, CO, isocyanide, ethylene, and so on. Recently coordinatively unsaturated dimer complexes of ruthenium,[39] such as $Cp^*Ru(\mu_2\text{-}SR)_3RuCp^*$,[40,41] $Cp^*Ru(\mu_2\text{-}SR)_2RuCp^*$,[42,43] $Cp^*Ru(\mu_2\text{-}S_2C_6H_4)RuCp^*$,[26] $Cp^*Ru(NCCH_3)(\mu\text{-}H)(\mu\text{-}N{=}CRH)Ru(NCCH_3)Cp^*$,[44] and $[Cp^*Ru(OMe)]_2$,[45] have been found generally to add donor molecules. Despite a rich chemistry of these electron deficient binuclear com-

(29) Sellmann, D.; Kleine-Kleffmann, U.; Zapf, L.; Huttner, G.; Zsolnai, L. *J. Organomet. Chem.* **1984**, *263*, 321.
(30) Sellmann, D.; Geck, M.; Knoch, F.; Ritter, G.; Dengler, J. *J. Am. Chem. Soc.* **1991**, *113*, 3819.
(31) Cowie, M.; Bennett, M. J. *Inorg. Chem.* **1976**, *15*, 1584.
(32) Oku, H.; Ueyama, N.; Kondo, M.; Nakamura, A. *Inorg. Chem.* **1994**, *33*, 209.
(33) Ueyama, N.; Oku, H.; Kondo, M.; Okamura, T.; Yoshinaga, N.; Nakamura, A. *Inorg. Chem.* **1996**, *35*, 643.
(34) Oku, H.; Ueyama, N.; Nakamura, A. *Chem. Lett.* **1996**, 31.
(35) Cowie, M.; Bennett, M. J. *Inorg. Chem.* **1976**, *15*, 1589.
(36) Cowie, M.; Bennett, M. J. *Inorg. Chem.* **1976**, *15*, 1595.
(37) Lopez-Castra, A.; Truter, M. R. *J. Chem. Soc.* **1963**, 1309. Robinson, W. T.; Hart, S. L., Jr.; Carpenter, G. B. *Inorg. Chem.* **1967**, *6*, 605. Weininger, M. S.; O'Connor, J. E.; Amma, E. L. *Inorg. Chem.* **1969**, *8*, 424.
(38) Degnan, I. A.; Behm, J.; Cook, M. R.; Herrmann, W. A. *Inorg. Chem.* **1991**, *30*, 2165.
(39) Hidai, M.; Mizobe, Y.; Matsuzaka, H. *J. Organomet. Chem.* **1994**, *473*, 1 and references cited therein.
(40) Dev, S.; Imagawa, K.; Mizobe, Y.; Cheng, G.; Wakatsuki, Y.; Yamazaki, H.; Hidai, M. *Organometallics* **1989**, *8*, 1232.
(41) Dev, S.; Mizobe, Y.; Hidai, M. *Inorg. Chem.* **1990**, *29*, 4797.
(42) Hörnig, A.; Rietmann, C.; Englert, U.; Wagner, T.; Kölle, U. *Chem. Ber.* **1993**, *126*, 2609.
(43) Koelle, U.; Rietmann, C.; Tjoe, J.; Wagner, T.; Englert, U. *Organometallics* **1995**, *14*, 703.

Table 2. Comparative Structural Data for $L_nM(SR)_2$-Type Thiolate Complexes

complex[a]	d(M−S),[b] Å	d(S−C), Å	⟨(S−M−S), deg	mode[b]	CN	ref
$CpMo(NO)(SPh)_2$	*exo* 2.345(1)	1.782(4)	112.66(5)	A	6	20
	exo 2.339(1)	1.779(5)				
$Tp^*Mo(O)(SPh)_2$	*exo* 2.380(2)		90.98(7)	B	6	21
	endo 2.383(2)					
$TpRe(O)(SPh)_2$	*exo* 2.312(2)	1.777(9)	89.6(1)	B	6	38
	endo 2.310(2)	1.80(1)				
2a	*exo* 2.269(7)	1.83(3)	88.0(3)	B	5[c]	this work
	endo 2.292(9)	1.78(2)				
2b	*exo* 2.263(7)	1.82(2)	89.0(2)	B	5[c]	this work
	endo 2.311(6)	1.77(2)				
3c	*exo* 2.259(1)	1.791(4)	86.74(4)	B	5[c]	this work
	endo 2.339(1)	1.777(4)				
$Cp^*Ir(SC_6F_5)_2$	*exo* 2.292(4)	1.764(13)	78.9(2)	A	5[c]	5
$Cp^*Ir(SC_6F_4H\text{-}p)_2$	*exo* 2.274(4)	1.773(13)	90.8(1)	B	5[c]	4, 5
	endo 2.323(4)	1.769(15)				

[a] Abbrevation: Cp* = η^5-pentamethylcyclopentadienyl; Tp = tris(pyrazolyl)hydroborate; Tp* = tris(3,5-dimethylpyrazolyl)hydroborate. [b] Notation according to Chart 1. [c] Two-legged piano stool geometry.

plexes, there is little investigation that deals with the reactions of monomeric coordinatively unsaturated ruthenium complexes. Reaction of the 16-electron complexes **2**−**4** with 2-electron donor molecules such as *tert*-butyl isocyanide, triethylphosphine, and carbon monoxide proceeded to give various 18-electron complexes with or without an arene ligand. Our results are closely related to those of the reported 16-electron ruthenium complexes $Cp^*RuX(PR_3)$ (R = isopropyl and cyclohexyl),[10,11] $[CpRu(Cy_2PCH_2CH_2PCy_2)]^+$,[46] and $Ru(CO)_2(PMe^tBu_2)_2$[47] together with the monomeric coordinatively unsaturated osmium complexes.[8]

Reaction with ^{t}BuNC. Treatment of **2b** with 10 equiv of ^{t}BuNC in THF afforded *trans*-$Ru(SXyl)_2(CN^tBu)_4$ (**8**) as yellow crystals in 78% yield. The ^{1}H NMR spectrum of **8** together with elemental analysis and FAB mass spectrum indicated that **8** was comprised of two 2,6-dimethylbenzenethiolate and four *tert*-butyl isocyanide ligands. The *trans* geometry of **8** was supported by its IR spectrum, one strong ν(CN) band at 2110 cm^{-1} and one weak ν(CN) band at 2060 cm^{-1} being closely related to the IR spectra of *trans*-$Ru(SnPh_3)_2(CN^tBu)_4$[48] and *trans*-$Ru(SiClMe_2)_2(CN^tBu)_4$.[48] The *trans*-ruthenium dithiolate complex **8** is likely to be a thermodynamic product, which is presumably derived from the isomerization of a kinetic product *cis*-ruthenium dithiolate complex through the Berry pseudorotation on pentacoordinated species such as $Ru(SXyl)_2(CN^tBu)_3$; a related crystallographically characterized example is $Fe(1,2\text{-}S_2C_6H_4)(PMe_3)_3$.[29]

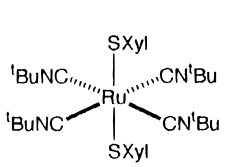

8

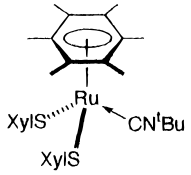

9c

A single-crystal X-ray structural determination of **8** (Figure 3) confirmed pseudooctahedral *trans* geometry. Selected bond distances and angles are summarized in Table 3. The Ru−S bond distances (2.472(3) and 2.453(3) Å) are longer by 0.1 Å than those of **2a**,**b** and **3c**, indicating the diminution of the S($p\pi$) → Ru($d\pi^*$) donation. These Ru−S bond distances are comparable to those found for an isoelectronic complex *trans*-$Ru(SPh)_2(dmpe)_2$ (dmpe = 1,2-bis(dimethylphosphino)ethane) (2.472(1) and 2.466(1) Å)[49] and *cis*,*cis*,*trans*-

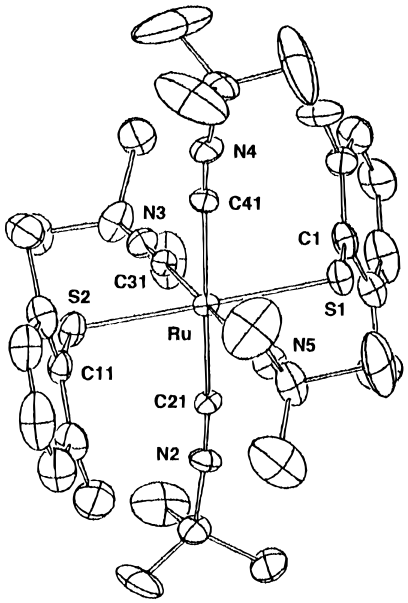

Figure 3. ORTEP drawing of **8** with the numbering scheme.

Table 3. Selected Bond Distances and Angles for 8

Bond Distances (Å)			
Ru−S1	2.472(3)	Ru−C41	2.02(1)
Ru−S2	2.453(3)	Ru−C51	1.97(1)
Ru−C21	1.959(8)	S1−C1	1.77(1)
Ru−C31	1.994(7)	S2−C11	1.79(1)
Bond Angles (deg)			
S1−Ru−S2	178.7(2)	C21−Ru−C31	85.5(4)
S1−Ru−C21	91.2(3)	C21−Ru−C41	178.4(6)
S1−Ru−C31	93.5(3)	C21−Ru−C51	95.5(4)
S1−Ru−C41	87.9(3)	C31−Ru−C41	93.2(4)
S1−Ru−C51	87.8(3)	C31−Ru−C51	178.3(5)
S2−Ru−C21	90.1(3)	C41−Ru−C51	85.8(4)
S2−Ru−C31	86.4(3)	Ru−S1−C1	110.3(4)
S2−Ru−C41	90.8(3)	Ru−S2−C11	114.1(4)
S2−Ru−C51	92.2(3)		

(44) Tada, K.; Oishi, M.; Suzuki, H.; Tanaka, M. *Organometallics* **1996**, *15*, 2422.
(45) Koelle, U.; Kang, B.-S.; Spaniol, T. P.; Englert, U. *Organometallics* **1992**, *11*, 249.
(46) Joslin, F. L.; Johnson, M. P.; Mague, J. T.; Roundhill, D. X. *Organometallics* **1991**, *10*, 2781.
(47) Ogasawara, M.; Macgregor, S. A.; Streib, W. E.; Folting, K.; Eisenstein, O.; Caulton, K. G. *J. Am. Chem. Soc.* **1995**, *117*, 8869.
(48) Corella, J. A., II; Thompson, R. L.; Cooper, N. J. *Angew. Chem., Int. Ed. Engl.* **1992**, *31*, 83.
(49) Field, L. D.; Hambley, T. W.; Yau, B. C. K. *Inorg. Chem.* **1994**, *33*, 2009.

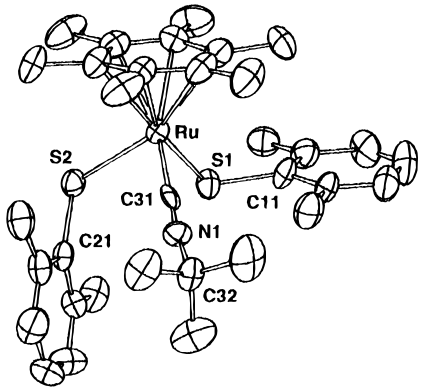

Figure 4. ORTEP drawing of **9c** with the numbering scheme.

$Ru(SC_6H_4Me\text{-}4)_2(CO)_2(PPh_3)_2$ (2.450(2) and 2.470(2) Å).[50] The bond distances between the ruthenium atom and carbon atoms of the isocyanide bound to the ruthenium lie in the range 1.959(8)−2.02(1) Å and are quite normal.

In the reaction course, an 18-electron isocyanide adduct (η^6-*p*-cymene)Ru(SXyl)$_2$(CN^{t}Bu) (**9b**) is assumed as an intermediate that further reacted with additional isocyanide through slipping of the η^6-*p*-cymene ligand and finally completely liberated the *p*-cymene ligand. In order to stabilize such an intermediate species, we used hexamethylbenzene complex **2c** by replacing the η^6-*p*-cymene ligand since hexamethylbenzene coordinates more strongly to ruthenium atom. Reaction of **2c** with an excess of ^{t}BuNC at room temperature proceeded smoothly, monitored by the change of the deep blue color of the solution to dark reddish brown. The complex **9c** was isolated in 53% yield as a reddish brown crystalline solid. Complex **9c** consists of ^{t}BuNC, a η^6-hexamethylbenzene ligand, and two 2,6-dimethylbenzenethiolate ligands, being proved by spectroscopic means along with a single-crystal X-ray analysis of **9c**. Complex **9c** exhibited a single CN stretching absorption at 2140 cm^{-1} in the IR spectrum, and this wavenumber is utterly normal for a terminal Ru−CNR ligand and significant π-back-bonding of the isocyanide ligand. FAB mass spectrum afforded a parent peak.

The structure of **9c** is depicted in Figure 4; selected distances and bond angles are listed in Table 4. The coordination sphere of the ruthenium center is comprised of an η^6-C_6Me_6 ligand, two sulfur atoms, and an isocyanide ligand, a three-legged piano stool geometry. Two thiolate ligands retain the "*endo-exo*" conformation **B**, the same as that of **2a**,**b** and **3c**. The two electron donor *tert*-butyl isocyanide stabilizes **9c** and makes the ruthenium center much more electron rich. Thus the Ru−C_6Me_6(centroid) distance (1.768 Å) in **9c** is greater by 0.066−0.095 Å than the analogous distance in **2a**,**b** and **3c**. The Ru−S bond distances (2.422(3) and 2.435(3) Å) in **9c** are significantly longer than those found for **2a**,**b** and **3c** but are normal for an 18-electron ruthenium thiolate complex.

Treatment of the dimer **5b** with an excess of ^{t}BuNC in THF gave yellow monomer **10** in 76% yield. The structure of **10** was determined on the basis of NMR spectroscopy and FAB mass and IR spectra, as well as elemental analysis. The IR spectrum of **10** showed four strong ν(CN) bands due to four *tert*-butyl isocyanide ligands, thus indicating a *cis* geometry of **10** in sharp contrast to the *trans* geometry of **8**. When 6 equiv of ^{t}BuNC was added to the solution of **5b** in THF, we obtained in 40% yield another yellow complex **11**. The FAB mass spectrum of **11** gave a parent peak and its fragmentation as a dimer. The ^{1}H NMR spectrum of **11** indicated three singlet signals at δ 1.02, 1.30 and 1.34 due to three magnetically nonequivalent *tert*-butyl moieties and the ABCD pattern due to four nonequivalent protons of a 1,2-benzenedithiolate ligand.

Table 4. Selected Bond Distances and Angles for 9c and 12c[a]

	9c	**12c**
Bond Distances (Å)		
Ru−S1	2.435(3)	2.353(2)
Ru−S2	2.422(3)	2.360(2)
Ru−C31	1.93(1)	1.932(5)
Ru−CEN	1.768	1.756
S1−C11	1.78(1)	1.747(6)
S2−C21	1.778(9)	1.764(6)
Bond Angles (deg)		
S1−Ru−S2	81.4(1)	85.67(6)
S1−Ru−C31	90.1(3)	89.3(2)
S2−Ru−C31	89.3(3)	88.7(2)
S1−Ru−CEN	130.7	124.9
S2−Ru−CEN	123.7	126.4
C31−Ru−CEN	127.4	128.7
Ru−S1−C11	118.6(4)	105.4(2)
Ru−S2−C21	115.0(3)	105.2(2)
Ru−C31−N1	175.6(9)	175.5(5)
C31−N1−C32	172.4(9)	177.0(5)

[a] CEN = the centroid of aromatic ring carbons, C1−C6, of the ligand.

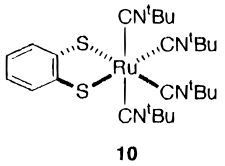

10

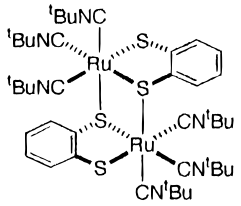

11

When **4c** was used, **12c** was obtained as reddish brown crystals in 74% yield. The ^{1}H NMR spectrum of **12c** exhibited two singlets at δ 1.19 and 2.09 due to the methyl moieties of the *tert*-butyl isocyanide and C_6Me_6 ligands, respectively. Proton signals due to the 1,2-benzenedithiolate ligand were observed as an AA′BB′ pattern. The IR spectrum of **12c** exhibited a strong absorption (2140 cm^{-1}) due to a ν(CN) band.

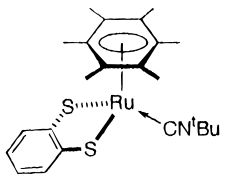

12c

Figure 5 shows the monomeric structure of **12c** that has one *tert*-butyl isocyanide. The selected bond distances and angles are summarized in Table 4. The structural features of **12c** are essentially equal to those found for **9c** except that **12c** has the chelating 1,2-benzenedithiolate ligand. The Ru−S bond distances (2.353(2) and 2.360(2) Å) of **12c** are longer by 0.1 Å than those found for **4c**. The distance (1.756 Å) between the ruthenium atom and the centroid of the aromatic

(50) Jessop, P. G.; Rettig, S. J.; Lee, C. L.; James, B. R. *Inorg. Chem.* **1991**, *30*, 4617.

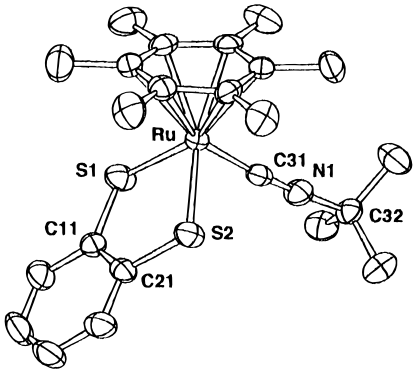

Figure 5. ORTEP drawing of **12c** with the numbering scheme.

carbons of the C_6Me_6 ligand is longer by 0.072 Å than that for **4c**.

Reaction with Trialkylphosphine. The reactions of **2a**,**b** with an excess of triethylphosphine, triphenylphosphine, or $P(OMe)_3$ resulted in the formation of complicated mixtures of unidentified phosphine complexes, whereas complexes **2c** and **3** did not react with those phosphine and phosphite molecules due to the steric bulkiness around the ruthenium atom in these complexes.

Trialkylphosphine is a more bulky ligand than isocyanide, and thus it is expected that only reaction with sterically less demanding complexes proceeds. We ultimately chose 1,2-benzenedithiolate complexes as starting ones. When an excess of triethylphosphine was added to a solution of **4c** in THF, the color of the solution gradually changed to deep brownish red, from which reddish orange crystals of **13c** were obtained upon cooling the saturated solution to −20 °C. Reaction of **5b** with an excess of PEt_3 in THF afforded also red crystals of **13b** in 59% yield. The $^{31}P\{^1H\}$ NMR of **13b**,**c** each exhibited singlet signals at δ 26.5 and 27.0, respectively. The ^1H NMR and FAB mass spectra supported the monomeric formulation. The structure of **13** is closely related to the phosphine adducts of iridium bis(thiolate) complexes $Cp^*Ir(SR)_2(PMe_3)$[6] and the osmium catecholate complex (η^6-*p*-cymene)Os-$(O_2C_6H_4)(PMe_3)$.[8]

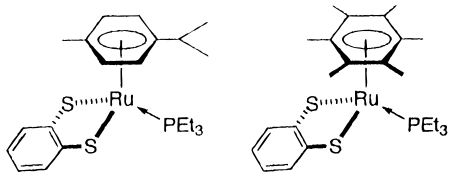

13b **13c**

Reaction with Carbon Monoxide. Treatment of **2b** with an atmospheric pressure of carbon monoxide in THF resulted in the formation of binuclear carbonyl complex **14** in 45% yield. The structure of **14** was determined on the basis of spectral data as well as elemental analysis. The ^1H NMR spectrum of **14** exhibited two sets of proton signals assignable to two kinds of 2,6-dimethylphenyl moieties in 1:3 ratio. The FAB mass spectrum gave a parent peak at *m*/*z* 755 due to a binuclear Ru(II) structure and its fragmentation by the consecutive loss of five CO ligands.

In the carbonylation of **2c** in THF, **15** was isolated in 45% yield. The ^1H NMR spectrum of **15** displayed a singlet at δ 1.49 due to the C_6Me_6 ligand in addition to the signals of two 2,6-dimethylphenyl moieties. The FAB mass spectrum indicated **15** to be monomeric and with one carbon monoxide bound to the ruthenium atom, in accordance with the strong ν(CO) band at 1965 cm^{-1} in the IR spectrum. Carbonylation of **2** is closely related to that of the 16-electron $Cp^*Ru(PR_3)X$ complexes, forming 18-electron species.[11]

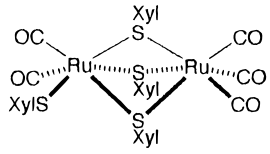

14

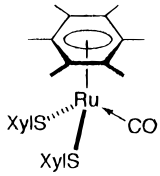

15

Conclusion

We prepared and characterized the complexes **2**, **3**, and **4c** as the first mononuclear 16-electron ruthenium(II) thiolate complexes. Our crystallographic study revealed the coordinative unsaturation in the steric sense around the ruthenium center in the two-legged piano stool geometry. The π-donation from the filled pπ orbital of the sulfur atom to the empty dπ orbital of the ruthenium atom is found to stabilize this unsaturation significantly. Complexes **2**−**4** still exhibit some coordinative unsaturation and thus are reactive toward various π-acceptor molecules such as isocyanide, phosphine, and carbon monoxide, depending upon the bulkiness around the ruthenium center. Thus, isocyanide and carbon monoxide are much more reactive than *tert*-phosphine. However, these complexes did not react with ethylene. These observations are rationalized by the efficient stabilization of the 16-electron ruthenium thiolate complexes by π-donation of the thiolate ligand.

Experimental Section

General Methods. All manipulations involving air- and moisture-sensitive organometallic compounds were carried out by the use of standard Schlenk techniques under argon atmosphere. Dichloromethane was purified by distillation under argon after drying over calcium hydride. Methanol was dried over magnesium alkoxide. THF, toluene, and hexane were dried over sodium benzophenone ketyl and then distilled before use. The complexes $[RuCl_2(\eta^6\text{-arene})]_2$ (**1**) were prepared according to the literature procedure.[51] 2,4,6-Triisopropylbenzenethiol was prepared according to the literature procedure[52] and then was oxidized by iodine to give the corresponding disulfide. 1,4-Cyclohexadiene was purchased from Nakalai Tesque, Inc. *p*-Mentha-1,5-diene and *tert*-butyl isocyanide were obtained from Tokyo Kasei Co., Ltd. Hexamethylbenzene was purchased from Lancaster. Ruthenium(III) chloride hydrate and 2,6-dimethylthiophenol were purchased from Aldrich.

Nuclear magnetic resonance [^1H (400 MHz and 270 MHz) and ^{31}P (36 MHz) NMR] spectra were measured on JEOL JNM-GX400, JEOL JNM-GSX-270, and JEOL EX-270 spectrometers. All ^1H NMR chemical shifts were reported in ppm relative to the protio impurity resonance as follows: chloroform-*d*, singlet at 7.27 ppm; benzene-d_6, singlet at 7.20 ppm. ^{31}P NMR chemical shifts were reported in ppm relative to external reference of 85% H_3PO_4 at 0.00 ppm. Other spectra were recorded by the use of the following instruments: IR, Hitachi 295; mass spectra, JEOL SX-102 spectrometer operating in

(51) Bennet, M. A.; Huang, T.-N.; Watheson, T. W.; Smith, A. K. *Inorg. Synth.* **1982**, *21*, 74.

(52) Blower, P. J.; Dilworth, J. R.; Hutchinson, J.; Nicholson, T.; Zubieta, J. A. *J. Chem. Soc., Dalton Trans.* **1985**, 2639.

the FAB$^+$ mode by using 3-nitrobenzyl alcohol (NBA) as a matrix; UV/vis spectra, Jasco Ubest-30 and Shimadzu UV-265FS. Elemental analyses were performed at the Elemental Analysis Center, Osaka University. All melting points were measured in sealed tubes and were not corrected.

Preparation of [(η^6-C_6H_6)Ru(SXyl)$_2$] (2a). Reaction of [$RuCl_2(\eta^6$-$C_6H_6)]_2$ (**1a**) (1.06 g, 1.61 mmol) with a suspension of sodium 2,6-dimethylbenzenethiolate prepared by the treatment of 2,6-dimethylbenzenethiol (0.95 mL, 7.13 mmol) and sodium methoxide (0.42 g, 7.70 mmol) in methanol (20 mL) afforded **2a** as dark greenish blue microcrystals (1.04 g, 71% yield), mp 175−177 °C (dec). ^{1}H NMR ($CDCl_3$, 30 °C): δ 2.46 (s, 12H, 2,6-$SC_6H_3Me_2$), 4.87 (s, 6H, C_6H_6), 7.03−7.16 (m, 6H, 2,6-$SC_6H_3Me_2$). FAB MS (NBA matrix): m/z 454 (M^+). UV/vis (THF): λ_{max} 698 (ϵ = 7900 M^{-1} cm^{-1}), 320 (28 400), 273 nm (36 800). Anal. Calcd for $C_{22}H_{24}RuS_2$: C, 58.24; H, 5.33. Found: C, 57.80; H, 5.32.

Preparation of [(η^6-*p*-cymene)Ru(SXyl)$_2$] (2b). To a suspension of sodium 2,6-dimethylbenzenethiolate [2,6-dimethylbenzenethiol (2.0 mL, 15.0 mmol) and sodium methoxide (1.01 g, 18.6 mmol)] in methanol (60 mL) was added [$RuCl_2$-(η^6-*p*-cymene)]$_2$ (**1b**) (2.31 g, 3.78 mmol) at room temperature. Rapid reaction proceeded to deposit deep blue crystalline solids. The supernatant solution was filtered off, and then the resulting product was washed with two portions of methanol (15 mL). Thus complex **2b** was isolated as deep blue microcrystals (3.50 g, 90% yield), mp 208−210 °C (dec). ^{1}H NMR ($CDCl_3$, 30 °C): δ 1.31 (d, J = 6.93 Hz, 6H, $CH_3C_6H_4CHMe_2$), 1.93 (s, 3H, $CH_3C_6H_4CHMe_2$), 2.35 (s, 12H, 2,6-$SC_6H_3Me_2$), 2.44 (m, 1H, $CH_3C_6H_4CHMe_2$), 4.80 (d, J = 6.27 Hz, 2H, $CH_3C_6H_4$-$CHMe_2$), 4.97 (d, J = 6.27 Hz, 2H, $CH_3C_6H_4CHMe_2$), 6.97−7.11 (m, 6H, 2,6-$SC_6H_3Me_2$). FAB MS (NBA matrix): m/z 510 (M^+). UV/vis ($CHCl_3$): λ_{max} 676 nm (ϵ = 3100 M^{-1} cm^{-1}). Anal. Calcd for $C_{26}H_{32}RuS_2$: C, 61.25; H, 6.33. Found: C, 61.13; H, 6.20.

Preparation of [(η^6-C_6Me_6)Ru(SXyl)$_2$] (2c). Similarly, reaction of [$RuCl_2(\eta^6$-$C_6Me_6)]_2$ (**1c**) (1.05 g, 1.56 mmol) with a suspension of sodium 2,6-dimethylbenzenethiolate (10.5 mmol) in methanol (20 mL) gave **2c** as a blue powder (1.33 g, 79% yield), mp 240−243 °C (dec). ^{1}H NMR ($CDCl_3$, 30 °C): δ 1.91 (s, 18H, C_6Me_6), 2.18 (s, 12H, 2,6-$SC_6H_3Me_2$), 6.89−7.00 (m, 6H, 2,6-$SC_6H_3Me_2$). FAB MS (NBA matrix): m/z 538 (M^+). UV/vis ($CHCl_3$): λ_{max} 660 (ϵ = 4200 M^{-1} cm^{-1}), 337 (20 400), 279 nm (44 200). Anal. Calcd for $C_{28}H_{36}RuS_2$: C, 62.52; H, 6.75. Found: C, 62.37; H, 6.64.

Preparation of [(η^6-C_6H_6)Ru(SC$_6$H$_2$(^{i}Pr)$_3$-2,4,6)$_2$] (3a). Complex **1a** (0.73 g, 1.47 mmol) was added to a solution of sodium 2,4,6-triisopropylbenzenethiolate derived from 2,4,6-triisopropylbenzene disulfide (1.38 g, 2.94 mmol) and sodium (0.14 g, 5.87 mmol) in THF (24 mL) at room temperature. The color of the reaction mixture changed rapidly from reddish brown to deep green. After the resulting mixture was stirred for 20 h, the solution was concentrated under reduced pressure and the resulting residue was recrystallized from THF−ethanol at −20 °C to afford **3a** as dark green needles (1.96 g, 83% yield), mp 130−132 °C (dec). ^{1}H NMR ($CDCl_3$, 35 °C): δ 1.21 (d, J = 6.68 Hz, 12H, *p*-CHMe_2 of $SC_6H_2(^iPr)_3$-2,4,6), 1.27 (d, J = 6.93 Hz, 24H, *o*-CHMe_2 of $SC_6H_2(^iPr)_3$-2,4,6), 2.90 (m, 2H, *p*-CH(CH_3)$_2$ of $SC_6H_2(^iPr)_3$-2,4,6), 3.75 (m, 4H, *o*-CH(CH_3)$_2$ of $SC_6H_2(^iPr)_3$-2,4,6), 4.92 (s, 6H, C_6H_6), 7.02 (s, 4H, SC_6H_2-(^{i}Pr)$_3$-2,4,6). FAB MS (NBA matrix): m/z 415 ($M^+ - SC_6H_2$-(^{i}Pr)$_3$-2,4,6). UV/vis (THF): λ_{max} 715 nm (ϵ = 4200 M^{-1} cm^{-1}). Anal. Calcd for $C_{36}H_{52}RuS_2$: C, 66.51; H, 8.06. Found: C, 66.26; H, 7.84.

Preparation of [(η^6-*p*-cymene)Ru(SC$_6$H$_2$(^{i}Pr)$_3$-2,4,6)$_2$] (3b). To a solution of sodium 2,4,6-triisopropylbenzenethiolate prepared by treatment of 2,4,6-triisopropylbenzene disulfide (1.63 g, 3.46 mmol) and sodium (0.16 g, 6.92 mmol) in THF (25 mL) was added **1b** (1.06 g, 1.73 mmol) at room temperature. Rapid reaction occurred to give a deep green solution. The solution was concentrated under reduced pressure, and the resulting residue was recrystallized from hexane at −20 °C to give **3b** as a dark blue green powder (1.87 g, 77% yield), mp 137−140 °C. ^{1}H NMR ($CDCl_3$, 35 °C): δ 1.17 (broad, 24H, *o*-CH(CH_3)$_2$ of $SC_6H_2(^iPr)_3$-2,4,6), 1.25 (d, J = 6.93 Hz, 12 H, *p*-CH(CH_3)$_2$ of $SC_6H_2(^iPr)_3$-2,4,6), 1.33 (d, J = 6.93 Hz, 6H, CH-(CH_3)$_2$ of *p*-cymene), 1.86 (s, 3H, *Me* of *p*-cymene), 2.43 (m, 2H, CH(CH_3)$_2$ of *p*-cymene), 2.86 (m, 2H, *p*-CH(CH_3)$_2$ of SC_6H_2-(^{i}Pr)$_3$-2,4,6), 3.57 (m, 4H, *o*-CH(CH_3)$_2$ of $SC_6H_2(^iPr)_3$-2,4,6), 4.88 and 5.05 (ABq, J = 6.1 Hz, 4H, aromatic protons of *p*-cymene), 6.95 (s, 4H, $SC_6H_2(^iPr)_3$-2,4,6). FAB MS (NBA matrix): m/z 707 (MH^+). UV/vis (THF): λ_{max} 686 nm (ϵ = 3600 M^{-1} cm^{-1}). Anal. Calcd for $C_{40}H_{60}RuS_2$: C, 68.03; H, 8.56. Found: C, 67.28; H, 8.57.

Preparation of [(η^6-C_6Me_6)Ru(SC$_6$H$_2$(^{i}Pr)$_3$-2,4,6)$_2$] (3c). To a solution of sodium 2,4,6-triisopropylbenzenethiolate prepared by treatment of 2,4,6-triisopropylbenzene disulfide (1.26 g, 2.68 mmol) and sodium (0.123 g, 5.35 mmol) in THF (25 mL) was added **1c** (0.67 g, 1.00 mmol) at room temperature. The reaction occurred immediately, and a deep green solution was obtained. After removal of all volatiles, recrystallization of the resulting residue from THF-ethanol at −20 °C afforded **3c** as dark green crystals (1.27 g, 87% yield), mp 178−181 °C. ^{1}H NMR ($CDCl_3$, 35 °C): δ 1.17 (broad, 36H, *Me* of $SC_6H_2(^iPr)_3$-2,4,6), 1.86 (s, 18H, C_6Me_6), 2.79 (m, 2H, *p*-CH(CH_3)$_2$ of $SC_6H_2(^iPr)_3$-2,4,6), 3.35 (m, 4H, *o*-CH(CH_3)$_2$ of $SC_6H_2(^iPr)_3$-2,4,6), 6.85 (s, 4H, $SC_6H_2(^iPr)_3$-2,4,6). FAB MS (NBA matrix): m/z 734 (M^+). UV/vis (THF): λ_{max} 669 nm (ϵ = 1100 M^{-1} cm^{-1}). Anal. Calcd for $C_{42}H_{64}RuS_2$: C, 68.70; H, 8.79. Found: C, 68.59; H, 8.87.

Preparation of [(η^6-C_6Me_6)Ru($S_2C_6H_4$)] (4c). To a suspension of **2c** (0.19 g, 0.36 mmol) in THF (20 mL) was added 2.1 equiv of sodium 1,2-benzenedithiolate (0.14 g, 0.75 mmol) at room temperature. The color of the solution turned to dark red within 10 min. After the reaction mixture was stirred for 2 h, precipitated salts were removed by centrifugation. The solution was concentrated under reduced pressure, and the resulting residue was recrystallized from a mixture of THF (7 mL) and hexane (3 mL) at −20 °C, affording **4c** as black crystals (66 mg, 46%), mp 262−265 °C. ^{1}H NMR ($CDCl_3$, 30 °C): δ 2.37 (s, 18H, C_6Me_6), 7.06 (m, ^3J = 5.94 Hz, ^4J = 3.30 Hz, 2H, 1,2-$S_2C_6H_4$), 7.91 (m, ^3J = 5.94 Hz, ^4J = 3.30 Hz, 2H, 1,2-$S_2C_6H_4$). FAB MS (NBA matrix): m/z 404 (M^+). UV/vis (THF): λ_{max} 563 (ϵ = 2200 M^{-1} cm^{-1}), 435 (10 500), 302 (9100), 257 nm (19 800). Anal. Calcd for $C_{18}H_{22}RuS_2$: C, 53.56; H, 5.49. Found: C, 53.38; H, 5.43.

Preparation of [(η^6-C_6H_6)Ru($S_2C_6H_4$)]$_2$ (5a). To a solution of **2a** (0.21 g, 0.46 mmol) in THF (20 mL) was added 1.5 equiv of sodium 1,2-benzenedithiolate (0.13 g, 0.70 mmol) at room temperature. From the reaction mixture, complex **5a** was immediately deposited as orange solids (70 mg, 48%), mp 190−194 °C (dec). Complex **5a** is in equilibrium with the corresponding monomer **4a** in solution. Low solubility in any common organic solvents hampered the purification of **5a**, and thus we could not obtain satisfactory elemental analysis. ^{1}H NMR ($CDCl_3$, 30 °C): **4a**, δ 5.87 (s, 6H, C_6H_6), 7.19 (dd, ^3J = 5.94 Hz, ^4J = 3.30 Hz, 2H, 1,2-$S_2C_6H_4$), 8.08 (dd, ^3J = 5.94 Hz, ^4J = 3.30 Hz, 2H, 1,2-$S_2C_6H_4$); **5a**, δ 4.97 (s, 12H, C_6H_6), 6.77 (dt, ^3J = 7.4 Hz, ^4J = 1.3 Hz, 2H, 1,2-$S_2C_6H_4$), 6.94 (dt, ^3J = 7.4 Hz, ^4J = 1.3 Hz, 2H, 1,2-$S_2C_6H_4$), 7.24 (dd, ^3J = 7.4 Hz, ^4J = 1.3 Hz, 2H, 1,2-$S_2C_6H_4$), 7.65 (dd, ^3J = 7.4 Hz, ^4J = 1.3 Hz, 2H, 1,2-$S_2C_6H_4$).

Preparation of [(η^6-*p*-cymene)Ru($S_2C_6H_4$)]$_2$ (5b). Treatment of **2b** (1.60 g, 3.15 mmol) in THF (60 mL) with 1.2 equiv of sodium 1,2-benzenedithiolate (0.72 g, 3.89 mmol) at room temperature gave **5b** as orange microcrystals (885 mg, 75%), mp 152−156 °C (dec). Complex **5b** is in equilibrium with the corresponding monomer **4b** in solution. ^{1}H NMR ($CDCl_3$, 30 °C): **4b**, δ 1.35 (d, J = 6.93 Hz, 6H, $CH_3C_6H_4CHMe_2$), 2.36 (s, 3H, $CH_3C_6H_4CHMe_2$), 2.72 (sept, 1H, $CH_3C_6H_4CHMe_2$), 5.70 and 5.73 (ABq, ^3J = 6.6 Hz, 4H, $CH_3C_6H_4CHMe_2$), 7.15 (dd, ^3J = 5.94 Hz, ^4J = 3.30 Hz, 2H, 1,2-$S_2C_6H_4$), 8.04 (dd, ^3J = 5.94 Hz, ^4J = 3.30 Hz, 2H, 1,2-$S_2C_6H_4$); **5b**, δ 1.18 and 1.21 (d, J = 6.93 Hz, 12H, $CH_3C_6H_4CHMe_2$), 2.20 (s, 6H, $CH_3C_6H_4$-$CHMe_2$), 2.89 (sept, 2H, $CH_3C_6H_4CHMe_2$), 4.26 (d, J = 5.38 Hz, 2H, $CH_3C_6H_4CHMe_2$), 4.38 (d, J = 5.38 Hz, 2H, $CH_3C_6H_4$-

$CHMe_2$), 4.46 (d, J = 5.94 Hz, 2H, $CH_3C_6H_4CHMe_2$), 4.85 (d, J = 5.94 Hz, 2H, $CH_3C_6H_4CHMe_2$), 6.74 (dt, ^3J = 7.6 Hz, ^4J = 1.3 Hz, 2H, 1,2-$S_2C_6H_4$), 6.91 (dt, ^3J = 7.6 Hz, ^4J = 1.3 Hz, 2H, 1,2-$S_2C_6H_4$), 7.20 (dd, ^3J = 7.6 Hz, ^4J = 1.3 Hz, 1,2-$S_2C_6H_4$), 7.60 (dd, ^3J = 7.6 Hz, ^4J = 1.3 Hz, 2H, 1,2-$S_2C_6H_4$). FAB MS (NBA matrix): m/z 752 (M^+ as a dimer), 618 [(M − *p*-cymene)$^+$, base peak], 376 (M − Ru − *p*-cymene − $C_6H_4S_2$)$^+$. UV/vis (THF) of the mixture of **4b** and **5b**: λ_{max} 298, 439, and 572 nm. Anal. Calcd for $C_{32}H_{36}Ru_2S_4$: C, 51.16; H, 4.83. Found: C, 51.34; H, 4.95.

Synthesis of *trans*-[Ru(SXyl)$_2$(CN^{t}Bu)$_4$] (8). To a solution of **2b** (0.13 g, 0.25 mmol) in THF (30 mL) was added an excess of ^{t}BuNC (0.28 mL, 2.48 mmol) at room temperature. After the reaction mixture was stirred overnight, the color of the solution turned to yellow. All volatiles were removed under reduced pressure. Recrystallization from a 1:1 mixture of THF and hexane at −20 °C afforded **8** as yellow crystals (136 mg, 78% yield), mp 184−186 °C (dec). ^{1}H NMR (C_6D_6, 30 °C): δ 1.13 (s, 36H, Me_3CNC), 2.99 (s, 12H, 2,6-$SC_6H_3Me_2$), 7.01−7.21 (m, 6H, 2,6-$SC_6H_3Me_2$). IR (Nujol): ν(CN)/cm^{-1} 2110 (s), 2060 (w). FAB MS (NBA matrix): m/z 708 (M^+), 625 (M − ^{t}BuNC)$^+$, 571 (M − SXyl)$^+$, 488 [(M − SXyl − ^{t}BuNC)$^+$, base peak]. UV/vis (THF): λ_{max} 317 nm (ϵ = 36 400 M^{-1} cm^{-1}). Anal. Calcd for $C_{36}H_{54}N_4RuS_2$: C, 61.06; H, 7.69; N, 7.91. Found: C, 61.09; H, 7.71; N, 7.93.

Synthesis of [(η^6-C$_6$Me$_6$)Ru(SXyl)$_2$(CN^{t}Bu)] (9c). To a suspension of **2c** (0.16 g, 0.29 mmol) in THF (40 mL) was added an excess of ^{t}BuNC (3.36 mmol) at room temperature. The color of the solution rapidly turned to dark reddish brown. After the reaction mixture was stirred overnight, all volatiles were removed under reduced pressure and then the resulting residue was dissolved in THF (5 mL). Recrystallization from THF−hexane (5 mL−3 mL) at −20 °C afforded **9c** as reddish brown crystals (96 mg, 53% yield), mp 150−155 °C (dec). ^{1}H NMR ($CDCl_3$, 30 °C): δ 1.25 (s, 9H, Me_3CNC), 1.90 (s, 18H, C_6Me_6), 2.44 (s, 12H, 2,6-$SC_6H_3Me_2$), 6.81−6.92 (m, 6H, 2,6-$SC_6H_3Me_2$). IR (Nujol): ν(CN)/cm^{-1} 2140 (s). FAB MS (NBA matrix): m/z 484 (M − SXyl)$^+$, 401 [(M − SXyl − ^{t}BuNC)$^+$, base peak]. UV/vis (THF): λ_{max} 298 nm (ϵ = 31 000 M^{-1} cm^{-1}). Anal. Calcd for $C_{33}H_{45}NRuS_2$: C, 63.82; H, 7.30; N, 2.26. Found: C, 63.15; H, 7.32; N, 2.26.

Synthesis of *cis*-[Ru(S$_2$C$_6$H$_4$)(CN^{t}Bu)$_4$] (10). To a solution of **5b** (69 mg, 0.09 mmol) in THF (17 mL) was added an excess of a 10% THF solution of ^{t}BuNC (2.1 mL, 1.86 mmol) at room temperature. While the reaction mixture was stirred for 2 h the color of the solution gradually turned to yellow. All volatiles were removed under reduced pressure, and the resulting residue was dissolved in THF (2 mL). Recrystallization from THF−hexane (2 mL−3 mL) at −20 °C afforded **10** as yellow microcrystals (80 mg, 76% yield), mp 258−260 °C (dec). ^{1}H NMR ($CDCl_3$, 30 °C): δ 1.08 (s, 36H, Me_3CNC), 6.90 (dd, ^3J = 5.61 Hz, ^4J = 3.30 Hz, 2H, 1,2-$S_2C_6H_4$), 8.06 (dd, ^3J = 5.61 Hz, ^4J = 3.30 Hz, 2H, 1,2-$S_2C_6H_4$). IR (Nujol): ν(CN)/cm^{-1} 2160 (s), 2100 (vs), 2080 (sh), 2040 (sh). FAB MS (NBA matrix): m/z 574 (M^+, base peak), 491 (M − ^{t}BuNC)$^+$, 434 (M − ^{t}BuNC − ^{t}Bu)$^+$. UV/vis (THF): λ_{max} 350 (ϵ = 6500 M^{-1} cm^{-1}), 308 nm (10 000). Anal. Calcd for $C_{26}H_{40}N_4RuS_2$: C, 54.41; H, 7.03; N, 9.76. Found: C, 54.10; H, 7.00; N, 9.65.

Synthesis of [Ru(μ-SC$_6$H$_4$S)(CN^{t}Bu)$_3$]$_2$ (11). Reaction of **5b** (66 mg, 0.09 mmol) in THF (20 mL) with 3 equiv of a 10% THF solution of ^{t}BuNC (0.62 mL, 0.55 mmol) at room temperature followed by recrystallization from THF−hexane (2 mL−2 mL) gave yellow crystals of **11** (69 mg, 40% yield), mp 265−268 °C (dec). ^{1}H NMR ($CDCl_3$, 30 °C): δ 1.02 (s, 18H, Me_3CNC), 1.30 (s, 18H, Me_3CNC), 1.34 (s, 18H, Me_3CNC), 6.48 (dt, ^3J = 7.6 Hz, ^4J = 1.3 Hz, 2H, 1,2-$S_2C_6H_4$), 6.67 (dt, ^3J = 7.6 Hz, ^4J = 1.3 Hz, 2H, 1,2-$S_2C_6H_4$), 7.16 (dd, ^3J = 7.6 Hz, ^4J = 1.3 Hz, 2H, 1,2-$S_2C_6H_4$), 7.58 (dd, ^3J = 7.6 Hz, ^4J = 1.3 Hz, 2H, 1,2-$S_2C_6H_4$). IR (Nujol): ν(CN)/cm^{-1} 2150 (s), 2100 (sh), 2060 (sh). FAB MS (NBA matrix): m/z 982 (M^+, base peak), 899 (M − ^{t}BuNC)$^+$, 816 (M − 2^{t}BuNC)$^+$, 733 (M − 3^{t}BuNC)$^+$. UV/vis (THF): λ_{max} 344 nm (ϵ = 11 300 M^{-1} cm^{-1}). Anal. Calcd for $C_{42}H_{62}N_6Ru_2S_4$: C, 51.39; H, 6.37; N, 8.56. Found: C, 51.92; H, 6.60; N, 8.95.

Synthesis of [(η^6-C$_6$Me$_6$)Ru(S$_2$C$_6$H$_4$)(CN^{t}Bu)] (12c). Treatment of **4c** (85 mg, 0.21 mmol) in THF (12 mL) with an excess of ^{t}BuNC (0.30 mL, 0.27 mmol) at room temperature gave **12c** as reddish orange crystals after recrystallization from THF (4 mL) and hexane (2 mL). Yield: 76 mg (74%), mp 150−156 °C (dec). ^{1}H NMR ($CDCl_3$, 30 °C): δ 1.19 (s, 9H, Me_3CNC), 2.09 (s, 18H, C_6Me_6), 6.55 (br, 2H, 1,2-$S_2C_6H_4$), 7.20 (dd, ^3J = 5.94 Hz, ^4J = 3.30 Hz, 2H, 1,2-$S_2C_6H_4$). IR (Nujol): ν(CN)/cm^{-1} 2140 (s). FAB MS (NBA matrix): m/z 487 (M^+), 404 [(M − ^{t}BuNC)$^+$, base peak]. UV/vis (THF): λ_{max} 352 (ϵ = 4300 M^{-1} cm^{-1}), 265 nm (17 200). Anal. Calcd for $C_{23}H_{31}NRuS_2$: C, 56.76; H, 6.42; N, 2.88. Found: C, 56.67; H, 6.39; N, 2.86.

Synthesis of [(η^6-*p*-cymene)Ru(S$_2$C$_6$H$_4$)(PEt$_3$)] (13b). To a solution of **5b** (71 mg, 0.10 mmol) in THF (20 mL) was added an excess of PEt_3 (0.28 mL, 1.90 mmol) at room temperature. The color of the reaction mixture rapidly turned to red, and then the reaction mixture was further stirred for 3 h. All volatiles were removed under reduced pressure, and the resulting residue was dissolved in THF (4 mL). Recrystallization from THF−hexane (4 mL−5 mL) at −20 °C afforded **13b** as red crystals (55 mg, 59% yield), mp 146−151 °C (dec). ^{1}H NMR ($CDCl_3$, 30 °C): δ 0.98−1.09 (m, 9H, P(CH_2CH_3)$_3$), 1.25 (d, 6H, J = 6.92 Hz, $CH_3C_6H_4CHMe_2$), 1.80−1.92 (m, 6H, P(CH_2CH_3)$_3$), 2.25 (s, 3H, $CH_3C_6H_4CHMe_2$), 2.91 (m, 1H, $CH_3C_6H_4CHMe_2$), 5.30 (d, J = 6.27 Hz, 2H, $CH_3C_6H_4CHMe_2$), 5.39 (d, J = 6.27 Hz, 2H, $CH_3C_6H_4CHMe_2$), 6.59 (dd, ^3J = 5.93 Hz, ^4J = 3.30 Hz, 2H, 1,2-$S_2C_6H_4$), 7.18 (dd, ^3J = 5.93 Hz, ^4J = 3.30, 2H, 1,2-$S_2C_6H_4$). ^{31}P{^{1}H} NMR (109.3 MHz, $CDCl_3$, 30 °C): δ 26.5 (s). FAB MS (NBA matrix): m/z 494 (M^+), 376 [(M − PEt_3)$^+$, base peak]. UV/vis (THF): λ_{max} 353 (ϵ = 5800 M^{-1} cm^{-1}), 271 nm (24 500). Anal. Calcd for $C_{22}H_{33}PRuS_2$: C, 53.51; H, 6.74. Found: C, 53.33; H, 6.78.

Synthesis of [(η^6-C$_6$Me$_6$)Ru(S$_2$C$_6$H$_4$)(PEt$_3$)] (13c). Reaction of **4c** (93 mg, 0.23 mmol) in THF (15 mL) with an excess of PEt_3 (0.34 mL, 2.30 mmol) at room temperature and followed by recrystallization from THF−hexane (10 mL−5 mL) afforded reddish orange crystals of **13c** (77 mg, 64% yield), mp 208−213 °C (dec). ^{1}H NMR ($CDCl_3$, 30 °C): δ 0.92−1.03 (m, 9H, P(CH_2CH_3)$_3$), 1.75−1.87 (m, 6H, P(CH_2CH_3)$_3$), 2.02 (s, 18H, C_6Me_6), 6.54 (dd, ^3J = 5.94 Hz, ^4J = 3.30 Hz, 2H, 1,2-$S_2C_6H_4$), 7.16 (dd, ^3J = 5.94 Hz, ^4J = 3.30 Hz, 2H, 1,2-$S_2C_6H_4$). ^{31}P{^{1}H} NMR (109.3 MHz, $CDCl_3$, 30 °C): δ 27.0 (s); FAB MS (NBA matrix): m/z 522 (M^+), 404 [(M − PEt_3)$^+$, base peak]. UV/vis (THF): λ_{max} 433 nm (ϵ = 740 M^{-1} cm^{-1}), 356 (4400), 278 (16 500). Anal. Calcd for $C_{24}H_{37}PRuS_2$: C, 55.24; H, 7.15. Found: C, 55.21; H, 7.18.

Synthesis of [(CO)$_2$(XyS)Ru(μ-SXyl)$_3$Ru(CO)$_3$] (14). A suspension of **2b** (0.15 g, 0.30 mmol) in THF (30 mL) was stirred overnight under an atmospheric pressure of carbon monoxide. The solution color turned gradually to reddish orange. The solvent was removed under reduced pressure, and the resulting residue was recrystallized from a mixture of THF (0.9 mL) and hexane (2 mL) at −20 °C to afford **14** as reddish orange crystalline solids (60 mg, 45% yield), mp 161−166 °C (dec). ^{1}H NMR ($CDCl_3$, 30 °C): δ 2.32 (s, 6H, 2,6-$SC_6H_3Me_2$), 3.00 (s, 18H, μ-2,6-$SC_6H_3Me_2$), 6.88 (s, 3H, 2,6-$SC_6H_3Me_2$), 7.12−7.22 (m, 9H, μ-2,6-$SC_6H_3Me_2$). IR (Nujol): ν(CO)/cm^{-1} 2100 (s), 2045 (s), 2020 (s), 1973 (s). FAB MS (NBA matrix): m/z 755 (M − SXyl)$^+$, 727 (M − SXyl − CO)$^+$, 699 (M − SXyl − 2CO)$^+$, 671 (M − SXyl − 3CO)$^+$, 643 (M − SXyl − 4CO)$^+$, 615 (M − SXyl − 5CO)$^+$, 534 (M − 2SXyl − 3CO)$^+$, 505 (M − 2SXyl − 4CO)$^+$, 477 [(M − 2SXyl − 5CO)$^+$, base peak]. UV/vis (CH_2Cl_2): λ_{max} 328 (ϵ = 18 400 M^{-1} cm^{-1}), 294 (19 100), 244 nm (28 000). Anal. Calcd for $C_{37}H_{36}O_5Ru_2S_4$: C, 49.86; H, 4.07. Found: C, 49.83; H, 4.33.

Synthesis of [(η^6-C$_6$Me$_6$)Ru(S$_2$C$_6$H$_4$)(CO)] (15). A suspension of **2c** (0.11 g, 0.21 mmol) in THF (20 mL) was stirred for 2 days under CO atmosphere. The color of the suspension turned to yellow brown. The solution was removed via syringe, and the resulting residue was washed with hexane (4 mL). An orange powder (54 mg, 45%) of **15** was obtained and dried

Table 5. Crystal and Refinement Data

complex	**2a**	**3c**	**4c**	**8**	**9c**	**12c**
formula	$C_{22}H_{24}RuS_2$	$C_{42}H_{64}RuS_2$	$C_{18}H_{22}RuS_2$	$C_{36}H_{54}N_4RuS_2$	$C_{33}H_{45}NRuS_2$	$C_{23}H_{31}NRuS_2$
fw	453.62	734.16	403.56	708.04	620.92	486.69
cryst system	orthorhombic	monoclinic	monoclinic	triclinic	monoclinic	monoclinic
space group	*Pbca* (No. 61)	$P2_1/c$ (No. 14)	$P2_1/n$ (No. 14)	*P*1 (No. 1)	$P2_1/a$ (No. 14)	$C2/c$ (No. 15)
a, Å	14.61(1)	18.472(6)	8.588(3)	9.488(2)	16.781(2)	26.060(6)
b, Å	19.598(5)	12.648(4)	14.170(3)	12.387(2)	9.554(3)	11.878(7)
c, Å	14.280(3)	19.905(4)	14.072(4)	9.305(3)	19.973(2)	17.715(5)
α, deg				111.81(2)		
β, deg		116.84(1)	94.09(3)	104.29(2)	107.45(1)	126.40(1)
γ, deg				81.20(2)		
Z	8	4	4	1	4	8
V, Å^3	4089(3)	4149(1)	1708.2(8)	981.6(5)	3055(1)	4413(3)
d_{calcd}, g cm^{-3}	1.474	1.175	1.569	1.198	1.350	1.465
radiation	Mo Kα (λ = 0.710 69 Å)	Mo Kα (λ = 0.710 69 Å)	Mo Kα (λ = 0.710 69 Å)	Mo Kα (λ = 0.710 69 Å)	Mo Kα (λ = 0.710 69 Å)	Mo Kα (λ = 0.710 69 Å)
reflcns measd	$+h,+k,+l$	$+h,+k,+l$	$+h,+k,\pm l$	$+h,\pm k,\pm l$	$+h,+k,\pm l$	$+h,+k,\pm l$
cryst size, cm	0.2 × 0.2 × 0.2	0.2 × 0.2 × 0.3	0.2 × 0.2 × 0.2	0.2 × 0.2 × 0.2	0.2 × 0.2 × 0.15	0.1 × 0.1 × 0.15
abs coeff, cm^{-1}	9.50	5.04	11.26	5.19	6.55	8.86
scan mode	$2\theta-\omega$	$2\theta-\omega$	$2\theta-\omega$	$2\theta-\omega$	$2\theta-\omega$	ω
temp, °C	23	20	23	23	23	23
$2\theta_{max}$, deg	55.1	55.0	55.1	60.1	55.1	55.1
data collcd	4115	10261	4382	6023	7771	5469
unique data	4115	9959 (R_{int} = 0.041)	4118 (R_{int} = 0.019)	5703 (R_{int} = 0.015)	7477 (R_{int} = 0.178)	5353 (R_{int} = 0.031)
no. of observns ($I > 3\sigma(I)$)	694	5678	2592	5254	3251	3096
no. of variables	117	407	207	385	371	245
R^a	0.066	0.043	0.034	0.027	0.066	0.041
$R_w{}^b$	0.060	0.029	0.037	0.032	0.076	0.044
GOF	1.58	2.64	1.30	1.20	2.12	1.32
Δ, e Å^{-3}	0.65 (max) −0.71 (min)	0.39 (max) −0.41 (min)	0.42 (max) −0.39 (min)	0.34 (max) −0.32 (min)	1.06 (max) −1.40 (min)	0.90 (max) −0.66 (min)

^{a} $R = \sum||F_o| - |F_c||/\sum|F_o|$. ^{b} $R_w = [\sum w(|F_o| - |F_c|)^2/\sum wF_o^2]^{1/2}$. $w = 1/\sigma^2(F_o)$. Function minimized: $\sum w(|F_o| - |F_c|)^2$.

under reduced pressure. Mp: 162−165 °C (dec). ^{1}H NMR (C_6D_6, 30 °C): δ 1.49 (s, 18H, C_6Me_6), 2.68 (s, 12H, 2,6-$SC_6H_3Me_2$), 7.07−7.12 (m, 6H, 2,6-$SC_6H_3Me_2$). IR (Nujol): ν(CO)/cm^{-1} 1965 (s). FAB MS (NBA matrix): *m*/*z* 429 (M − SXyl)$^+$, 401 (M − SXyl − CO)$^+$. UV/vis (CH_2Cl_2): λ_{max} 320 (ϵ = 12 300 M^{-1} cm^{-1}), 289 nm (12 800). Anal. Calcd for $C_{29}H_{36}ORuS_2$: C, 61.56; H, 6.41. Found: C, 61.11; H, 6.40.

Crystallographic Data Collection and Structure Determinations of 2a, 3c, 4c, 8, 9c, and 12c. Data Collection. Suitable crystals were mounted in glass capillaries under an argon atmosphere. Data for three complexes were collected by a Rigaku AFC-5R diffractometer with a graphite-monochromated Mo Kα radiation and a 12 kW rotating anode generator. The incident beam collimator was 1.0 mm, and the crystal to detector distance was 285 mm. Cell constants and an orientation matrix for data collection, obtained from a least-squares refinement using the setting angles of 25 carefully centered reflections, corresponded to the cells with dimensions listed in Table 5, where details of the data collection were summarized. The weak reflections ($I < 10\sigma(I)$) were rescanned (maximum of 2 rescans), and the counts were accumulated to ensure good counting statistics. Stationary background counts were recorded on each side of the reflection. The ratio of peak counting time to background counting time was 2:1. Three standard reflections were chosen and monitored every 100 reflections.

Data Reduction. An empirical absorption correction based on azimuthal scans of several reflections was applied. The data were corrected for Lorentz and polarization effects. The decay of intensities of three representative reflections for **2a** was −3.7%, and thus a linear correction factor was applied to the decay of the observed data. No significant decay was observed for complexes **3c**, **4c**, **8**, **9c**, and **12c**.

Structure Determination and Refinement. All calculations were performed using a TEXSAN crystallographic software package of the Molecular Structure Corp. Measured nonequivalent reflections with $I > 3.0\sigma(I)$ were used for the structure determination. The structures of **2a** and **8** were solved by direct methods (MITHRIL), the structure of **3c** was solved by direct methods (SHELXS86),[53] the structures of **4c** and **9c** were solved by the heavy-atom Patterson method (PHASE), and the structure of **12c** was solved by the heavy-atom Patterson method (PATTY). These were expanded using Fourier techniques. For complexes **3c**, **4c**, **8**, **9c**, and **12c**, all non-hydrogen atoms were refined anisotropically, while for complex **2a** a ruthenium atom and two sulfur atoms were refined anisotropically and all carbon atoms were refined isotropically since the collected reflection data were quite poor and the number of significant data was too little. In the final refinement cycle (full-matrix least-squares refinement) of all complexes, hydrogen atom coordinates were included at idealized positions and were given the same temperature factor as that of the carbon atom to which they were bonded. For all atoms, neutral atom scattering factors were taken from ref 54.

Acknowledgment. K.M. is grateful for financial support from the Ministry of Education, Science, Sports, and Culture of Japan (Nos. 07651057 and 08640711). This work was also supported by the Kurata Foundation.

Supporting Information Available: Listings of atomic coordinates and *B* values, bond distances and angles, and anisotropic thermal parameters for complexes **2a**, **3c**, **4c**, **8**, **9c**, and **12c** and an Arrhenius plot for the equilibrium between **4b** and **5b** (60 pages). Ordering information is given on any current masthead page.

OM960759C

(53) Sheldrick, G. M. In *Crystallographic Computing 3*; Sheldrick, G. M., Kruger, C., Goddard, R., Eds.; Oxford University Press: Oxford, U.K., 1985; p 179.
(54) Cromer, D. T.; Waber, J. T. *International Tables for X-ray Crystallography*; The Kynoch Press: Birmingham, England, 1974; Vol. IV.